AN ELASTIC-WAVE-BASED IMAGING METHOD FOR SCANNING THE DEFECTS INSIDE THE STRUCTURE

Jian-Hua Tong [1], Shu-Tao Liao [2]

[1] Department of Computer Science and Information Engineering, Hungkung University
[2] Department of Civil Engineering, Chung Hua University

Abstract

In this paper, a new nondestructive testing method utilizing elastic waves for imaging possible voids or defects in concrete structures is proposed. This method integrates the point-source/point receiver scheme with SAFT process to achieve the effect like scanning with a phase array system. This method is also equipped with large functioning depth because of the high energy feature that elastic waves usually possess over traditional ultrasound. Both numerical simulations and experimental tests were carried out to explore the capabilities of this method in revealing single or multiple defects implied in a matrix material. The results from numerical simulations indicate that this method can clearly reveal the number of the voids or defects and their locations and front-end profiles. Both the results from the numerical simulations and the experimental test indicate that this elastic-wave-based method exhibits high potential in inspecting the defects of in-situ concrete structures by imaging.

1. Introduction

Among the present nondestructive testing (NDT) technologies for civil engineering [1-7], the elastic-wave-based application always plays a very important role. The point-source/point-receiver scheme is especially suitable for the inspection of on-site civil infrastructures. It overcomes the limitation of transmission distance caused by the nature of the traditional ultrasonic probing, which is featured by low output power. In view of these developments, it can be expected that the elastic-wave-based method, used in conjunction with the point-source/point-receiver scheme, is a good NDT solution for evaluating the integrity of in-situ concrete infrastructures. However, when these methods are applied to detect the defects inside the concrete structures, especially with complex boundary conditions or multiple inclusions, successful results are usually hard to obtain with analyzing just one response signal.

In the application of medical ultrasound, phase array probing is often adopted to enhance the S/N ratio of the received signal by focusing the energy at a specific location in the specimen. Some researchers tried to use the ultrasonic phase array probing as a NDT technique for application and indeed successfully discovered the defects inside the concrete specimen by this imaging method [8-11]. It seems that phase array probing technique could be a good idea as a NDT method in civil engineering. However, it takes a lot of modifications to make this method applicable in the use of in-situ concrete structures. It is important to note that the energy of ultrasound decayed so quickly in concrete that the effective functioning depth will be very limited. Besides, the cost is too high and the size of the apparatus will be too large to be used for civil engineering. Therefore it is a great need to develop a new imaging method for scanning the defects inside in-situ concrete structures.

The synthetic aperture focusing technique (SAFT) is often used as a signal processing strategy in ultrasonic testing as a NDT method for metallic materials. A pulse-echo probe is utilized to generate the ultrasonic wave and then the reflected signal is received. Shifting and superposing the response signals recorded by multiple pulse-echo experiments, good results of high S/N ratio can be obtained as those obtained with the phase array system [12-14]. As mentioned above, the point-source/ point-receiver scheme has been widely used in the NDT field for civil engineering. This method is equipped with the advantages of generating high energy wave, increasing the effective inspecting depth and reducing the cost and size of the apparatus. In this paper, a new elastic-wave-based imaging method, which combines the point-source/ point-receiver scheme and SAFT method, will be introduced. Good results were obtained not only from the numerical simulation but also from the experiment. The defects embedded in the concrete

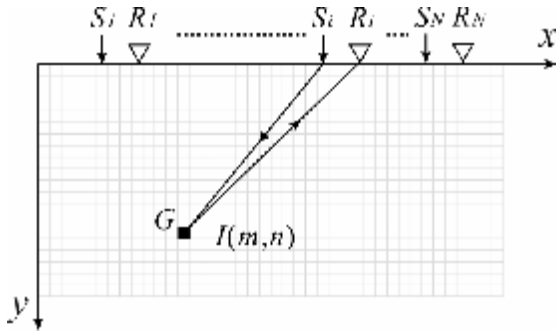

Fig. 1. Schematic showing the implementation of impact-and-receive operations and meshing of specimen for image processing with SAFT.

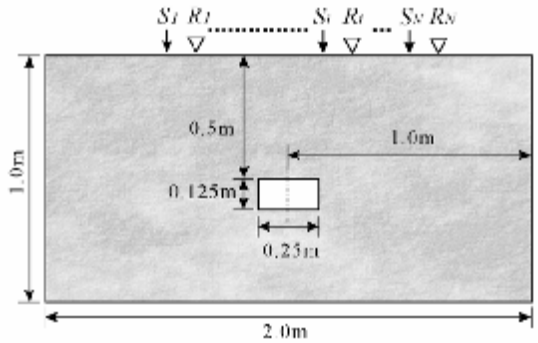

Fig. 2. Dimensions of concrete specimen with rectangular void bar for the study of numerical simulation.

specimen can be clearly identified from the image processed with this new scheme. It could be a practical and effective NDT method for defect inspection on civil infrastructures.

2. Principle of imaging

In the traditional SAFT-imaging method, the measurement is performed just with one ultrasonic probe. To match the present NDT measuring scheme in civil engineering, the measurement in this paper is replaced with a point-source/point-receiver set with a certain offset. Shown in Fig. 1 is a concrete specimen to be tested. A series of impact-and-receive operations is performed on the free surface of the specimen. Let S_i and R_i represent the locations of a set of the source and receiver for the i-th measurement. Furthermore let $T_i(t)$ be the magnitude of the response signal recorded at R_i for this measurement. The domain of the specimen is then divided into mesh grids on paper. An image intensity $I(m,n)$ can be assigned to each grid based on the following calculation

$$I(m,n) = \frac{1}{N}\sum_{i=1}^{N} T_i(t_i) \quad , \quad t_i = \frac{\left|\overrightarrow{S_iG}\right| + \left|\overrightarrow{GR_i}\right|}{C_P} \qquad (1)$$

where m and n specify that the grid is on the m-th row and n-th column, N is the total number of the measurements and C_P is the propagating velocity of the longitudinal wave.

The reflection can be found in the response time history if it can be sensed by the transducer. In general case, however, there are so many reflected signals from the boundaries and defects that determining the location of a defect from the complex trace is very hard. Besides, the dimension of the defect cannot be obtained from a single response signal. In this imaging process, the geometric information of a defect can be recovered not only from one set of the response signals but from all of them. In the summation, the intensity of the grids I associated with defects or interfaces will be enhanced whereas that of the grids associated with uniform matrix will be reduced due to cross interference. The rest of the scheme is to map the intensity value of each grid to a color or brightness on the grayscale. With this image processing scheme, the defects and interfaces implied in the matrix material can be exposed. In this paper, high image density associated with defects and interfaces will be displayed with bright white while low density associated with uniform matrix will be displayed with dark black. The resultant image will be similar to that scanned with a phased array system.

3. Results of Numerical Simulation

In this paper, a finite difference program for solving 2-D plane-strain problems was used as the numerical simulating tool to verify the practicability of the new method mentioned above.

3.1. Displacement image of Single Defect

First consider a concrete block with a rectangular void as a specimen, as shown in Fig. 2. The Lame′ constant, , , and mass density of the concrete block are 6.890×10^9 N/m^2, 1.379×10^{10} N/m^2, and 2300 kg/m^3 so that the propagating velocity of the longitudinal wave is 3871m/s. A series of impact-and-receive operations are then performed on the top surface of the block, as indicated by $\{S_1, R_1\}\ldots\ \{S_i, R_i\}$, etc. on the figure. The impact is assumed to be generated by dropping a steel ball of 6mm in diameter and it is simulated by a half of the $\sin^{3/2} t$ force-time function with a contact duration of 30 s [20]. The response signals of the displacement and velocity recorded by the nearby receiver on the surface are obtained for further process.

Assume that the first impact S_1 is applied at 0.5m from the left side of the block. The distance between the source and

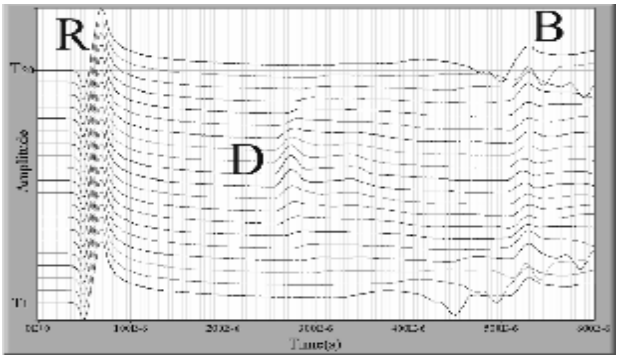

Fig. 3. B-scan displacement diagram of concrete specimen with single rectangular void bar in numerical simulation.

the receiver is fixed at 0.1m. After the response is measured, the impacting source is moved 0.1m to the right for the next measurement.

Shown in Fig. 3 is the B-scan diagram of the 20 displacement signals in the vertical direction. These 20 traces are placed in upward order along the *y*-axis. The fluctuations which are marked with "R" are associated with the arrival of Rayleigh waves. Those marked with "B" are associated with the reflections from the bottom surface. These two kinds of signals can be observed on all recorded traces. The arrival time and the amplitude of each of these two kinds are almost the same because of the same traveling distance. However, some fluctuations come into interfering with the reflection signals from the bottom in those traces measured near the left and right sides of the block. This is because that the Rayleigh waves reflecting from the side boundaries have come into the stage. The fluctuations marked with "D" are associated with the reflections from the defect. It is seen that clear reflections from the defect can be observed in those traces measured around the central region of the top surface. The farther the measurement is made away from the center of the top surface, the smaller the amplitude of the reflection from the defect, and the larger the delay of the arrival time. Using the algorithm and image processing technique implied in SAFT and Equation (1) to manipulate these 20 traces, a scan-like image can be obtained as shown in Fig. 4. In this figure, a bright strip can be found near the top free surface. It does not imply an interface but the ghost image caused by Rayleigh wave. The bright strip in the center, as enclosed by a dashed rectangle, indicates that there exists a defect. From the figure, not only the location but also the width of the defect can be observed. It should be noted that the majority of the reflected waves associated with the defect corresponds to the reflections on the top surface of the defect could be sensed by receivers and therefore only the upper boundary of the

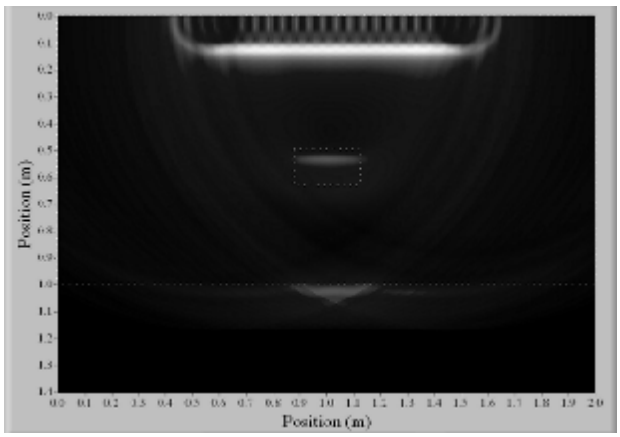

Fig. 4. Original SAFT image generated from displacement responses of concrete specimen with single rectangular void.

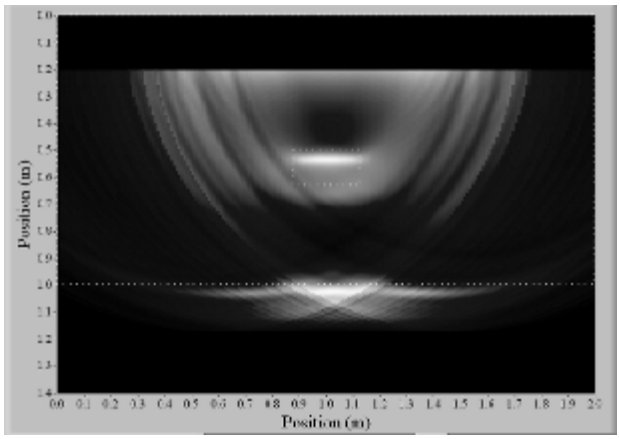

Fig .5. Revised SAFT image generated from displacement responses of concrete specimen with single rectangular void bar.

void can be identified from the image with this method. The outer boundaries of the specimen are also indicated with a dashed rectangle in Fig. 4. A long bright strip associated with the bottom of the specimen can also be seen in the image. The two bright curves intersecting at the central bottom of the image are generated by the reflected Rayleigh waves.

It is worth to note that the amplitude of the Rayleigh wave is relatively larger than that of the signals reflected from the defect. The dynamic range of the image intensity is so large that the void cannot be clearly revealed because the contrast of the image representing the void is compressed. To enhance the contrast of the defect and the matrix, the image region of a horizontal strip with a thickness of 0.2m below the free surface is then erased to a dark area. The contrast of void and matrix is evidently enhanced in the remnant image once the influence of Rayleigh wave is eliminated. It is obvious that the location, the front-end geometry of the defect and the bottom boundary of the specimen can be obtained more easily with this processed image.

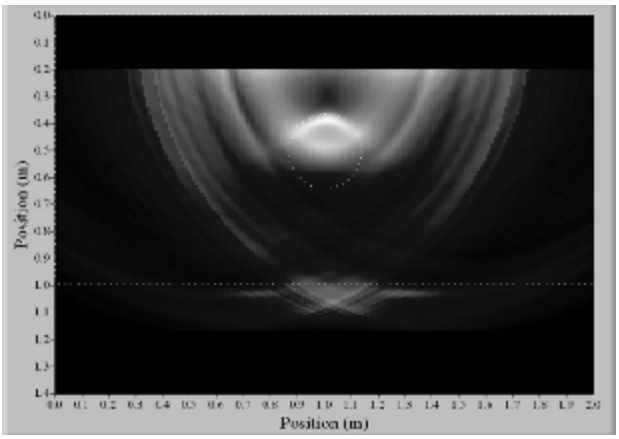

Fig. 6. Revised SAFT image generated from displacement responses of concrete specimen with single circular void bar.

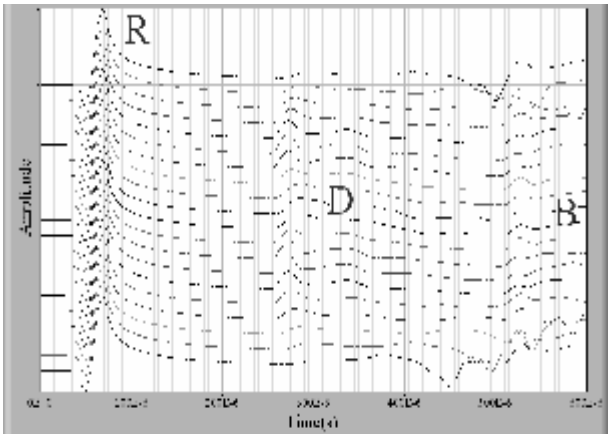

Fig. 7. B-scan displacement diagram of concrete specimen with two rectangular void bars.

Next consider that the cross section of the void is changed from a rectangle to a circle with 0.3m in diameter. This circle is centered at a depth of 0.5m from the top free surface. After the same image processing work, a scan-like picture with the influence of Rayleigh wave being eliminated is shown in Fig. 6. In the figure the cross section of the void is indicated by a dashed circle. From the result, it is seen that not only the location but also the upper part of the void can be clearly observed. It can be seen that the results obtained with the method proposed in this paper is much more readable than the traditional B-scan diagram. The resultant image can provide quite complete information of the defect such as its location and geometry.

3.2. Displacement Image of Multiple Defects

Now consider two voids in the same specimen as before. Both the two voids are the same size as the single one discussed before. Using numerical simulation, the displacement B-scan diagram of this specimen is shown in Fig. 7. It is not hard to identify the arrival of the waves reflected from the defects. However, it is not practical to tell the number of defects directly from this displacement time history. Using the same image processing scheme as before, the final scan-like image is shown in Fig. 8. Now two bright strips indicating the upper boundaries of the two voids can be clearly identified in the figure. The actual locations and cross sections of these two voids are also indicated by two dashed rectangles in the figure for comparison. It can be seen that the bright zones coincide with the substantial voids. The bottom of the specimen could also be found in the image. The bottom reflection is not as clear as that in Fig.5 of a single void case. This is because that most of the energy of the traveling waves is

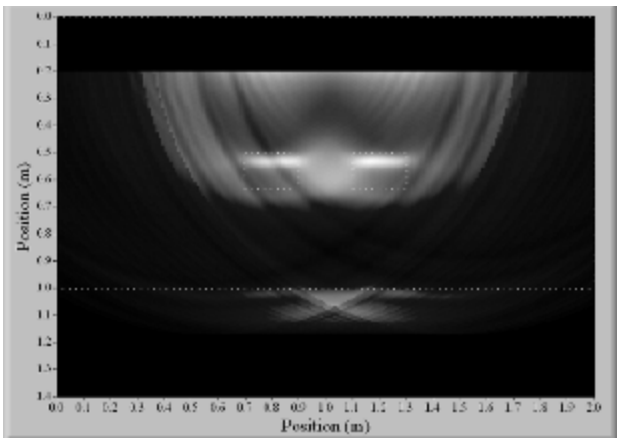

Fig. 8. Revised SAFT image generated from displacement responses of concrete specimen with two rectangular void bars.

reflected back by the defects and only a small part of it can reach the bottom of the specimen. It is worth noting that these two voids could not be distinguished directly from the traditional B-scan diagram even though the reflected wave does appear in the response traces. It is the proposed image processing scheme which makes the identification work so easy and straightforward.

3.3. Influence of Accuracy in Wave Velocity

It is very hard to accurately define the velocity of the elastic wave propagating inside a concrete structure because the composite material is inhomogeneous. Since concrete is a mixture of cement paste and aggregates, the mechanical properties must suffer a variation in locations. Therefore the wave velocity measured on any location, usually by ultrasonic or transient elastic wave methods, can only have local representation. With such consideration, the influence of accuracy in wave velocity used for calculation on the proposed method should be discussed. To explore the effect, it is assumed that the wave velocity measured on the free surface of the concrete

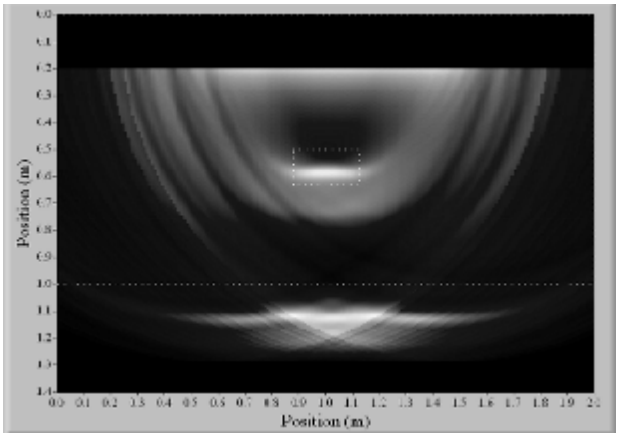

Fig. 9. Revised SAFT image generated from displacement responses of concrete specimen with wave velocity being 10% higher than actual value and single rectangular void bar.

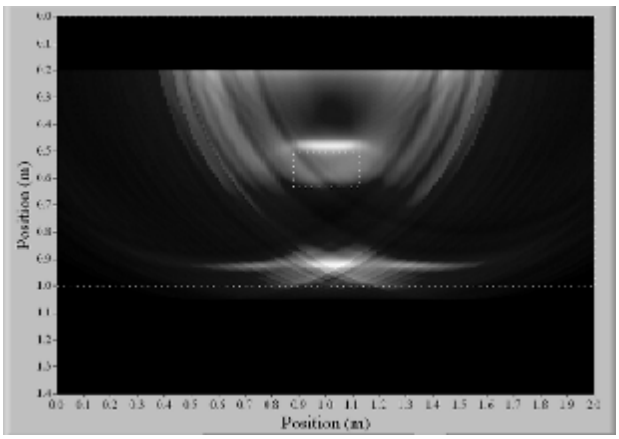

Fig. 10. Revised SAFT image generated from displacement responses of concrete specimen with wave velocity being 10% lower than actual value and single rectangular void bar.

block is actually lower or higher than that used in the numerical simulation model. In other words, the specimen in the numerical model is totally the same as shown in Fig. 2 and therefore the displacement responses should be the same as in Fig. 3. However as go onto image processing stage, incorrect wave velocity C_P is assumed to be used for carrying out the calculation implied in Eq. (1). Shown in Fig. 9 and Fig. 10 are the scan-like images obtained from response traces in Fig. 3 by using wave velocity 10% higher and 10% lower than actual value, respectively. As shown in Fig. 9, it is quite obvious that the inaccuracy of wave velocity does not damage the image. The only variation from Fig. 5 is that the bright strips representing the defect and bottom boundary become deeper owing to that the higher wave velocity was adopted for calculation. On the contrary, the bright strips become shallower as shown in Fig. 10 while the adopted wave velocity is lower than actual value. These results lead to the conclusion that a few inaccuracy of wave velocity used for calculation

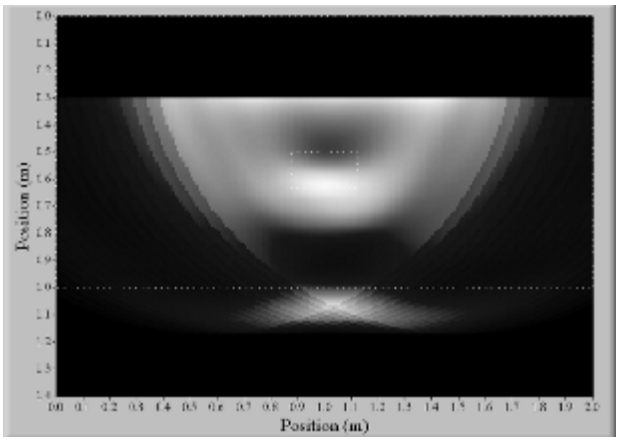

Fig. 11. Revised SAFT image generated from displacement responses of concrete specimen with single rectangular void bar and the impacting duration being increased from 30 s to 94 s.

does not seriously damage the image but the location of reflection surface will a little bit be shifted.

3.4. Influence of wavelength

In order to understand how the wavelength affects the image quality, the contact duration of the force-time function is increased from 30 s to 94 s so that elastic waves of longer wavelength may be introduced into the specimen. The resultant image is shown in Fig. 11. Comparing Fig. 11 and Fig. 5 indicates that the defect and the bottom boundary are still identifiable in Fig. 11. However, the location of the void moves down a little and the corresponding strips become blurrier than that as shown in Fig. 5. This phenomenon, which reduces the resolution of the image, results from the fact that a wave with high wavelength or low frequency can detect objects of large dimension but not the detail, or vice versa. In this case, the wavelength of the longitudinal wave is increased to about 0.7m, which is quite large compared with the width of the defect, 0.2m. Furthermore, larger wavelength implies that the waveform associated with the reflections is less steep and therefore the bright strip associated with the void is moved a little down than it was in Fig. 5. This is an important note when low frequency wave is used to make the detection.

4. Experimental Results

To verify the new imaging method proposed in this paper, a defective concrete block is placed for experiment, as shown in Fig. 12. A horizontal void bar, extending through the whole width of the block, is placed at the center of the block.

The experiment was then carried out with a series of impact-and-receive operations on the top surface of the

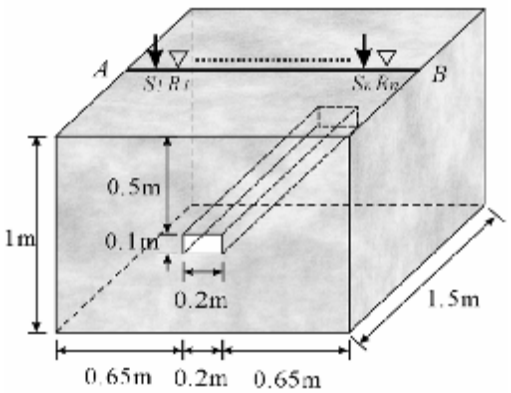

Fig. 12. Dimensions of concrete specimen with rectangular void bar for experimental study.

concrete block along the sampling line AB indicated in Fig. 12. The distance between the impacting source and the receiver is always set to be 10cm and the distance to move from the current impacting point to the next one is 5cm. The first measurement was made at 5cm from the side surface of the block. The elastic wave was generated by the impact of a steel ball falling at a height of 15cm. A vertical-polarized PZT transducer, placed on the top surface of the concrete block, was used to record the displacement response in the vertical direction. There were 25 displacement traces recorded for the imaging process. The longitudinal wave velocity is 3200m/s, which is measured on the top surface of the concrete block by using the horizontally polarized conical transducers [2], [21].

4.1. 19mm Steel Ball Impact

The B-scan diagram shown in Fig. 13 is the 25 displacement traces recorded when the concrete block is impacted by a falling steel ball of 19mm in diameter. The dashed vertical line marked with 'R' indicates the arrival time of Rayleigh wave. The other two dashed vertical lines marked with 'D' and 'B' represent the arrival times of the longitudinal waves reflected from the top surface of the void and the bottom surface of the concrete block, respectively. The inclined dashed lines marked with 'RR' indicate the arrivals of the Rayleigh waves reflected from the side surfaces of the concrete block.

Using the image processing scheme to process the 25 traces in Fig. 13, a scan-like picture is shown in Fig. 14. It can be seen that a bright zone appears at the place of the void. Another bright strip corresponding to the bottom boundary of the specimen can also be found beneath the defect.

4.2. 8mm Steel Ball Impact

To study how the wavelength of the propagating waves affects the resolution of the image, the diameter of the steel ball is reduced from 19mm to 8mm so that the wavelength of the introduced wave may be reduced. The B-scan diagram obtained with this source is shown in Fig. 15. Comparing Fig. 15 and Fig. 13 indicates that small oscillations become more obvious in these traces and thus marking the arrivals of the reflected waves is not as easy as that in Fig. 13. Because of these oscillations, the contrast of the processed image, as shown in Fig. 16, is no longer as high as before. Nevertheless, the bright zones corresponding to the void and the bottom of the specimen can still be identified in this image.

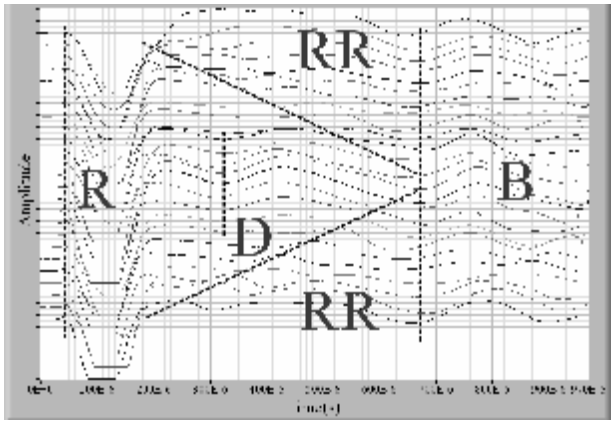

Fig. 13. B-scan displacement diagram of experimental concrete specimen subjected to an impacting of 19mm steel ball.

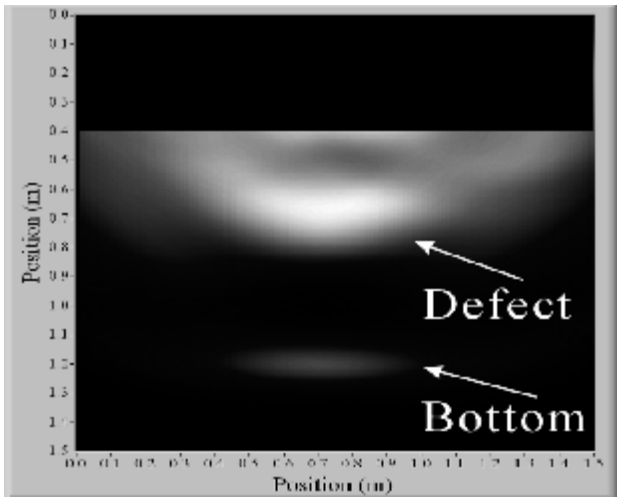

Fig. 14. Revised SAFT image generated from responses of experimental concrete specimen subjected to an impacting of 19mm steel ball.

4.3. Discussion

It can be seen from the experimental results that locating and identifying possible defects in concrete structure is much more easy and straightforward by the image generated with the proposed method than by the traditional B-scan diagram. From numerical simulation, it

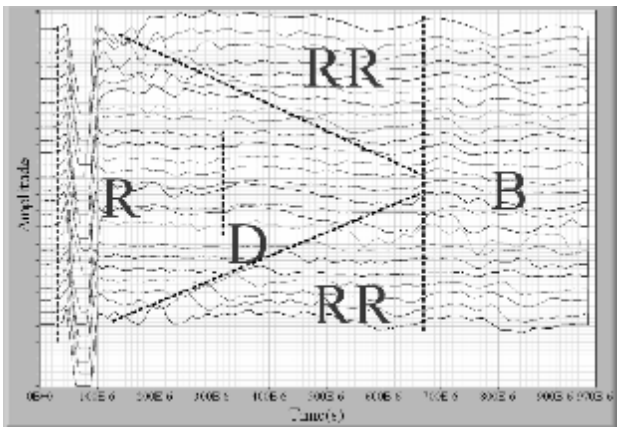

Fig. 15. B-scan displacement diagram of experimental concrete specimen subjected to an impacting of 8mm steel ball.

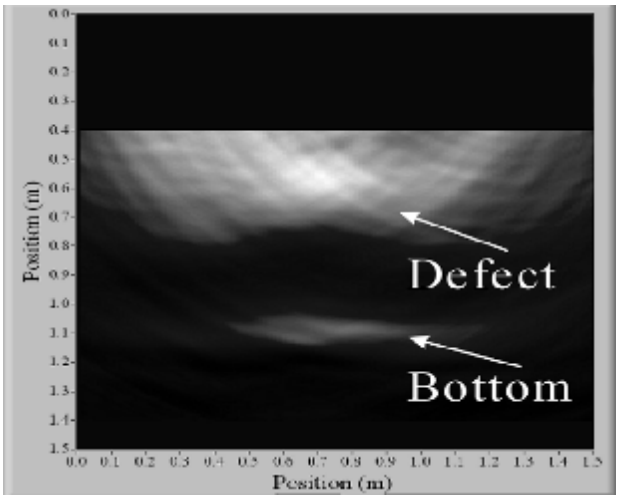

Fig. 16. Revised SAFT image generated from responses of experimental concrete specimen subjected to an impacting of 8mm steel ball.

is noteworthy that the resolution of the image generated with high frequency wave should be higher than that with low frequency wave. However, the validity of this conclusion is confined by the fact that in practice concrete is a mixture of cement paste and aggregates and thus it cannot be regarded as a homogeneous material. If the wavelength of the introduced wave is too small, scattering on the aggregates may deteriorate the resolution of the image. This phenomenon can be observed in the experimental results. To have good scanning results, the wave length of the elastic wave used in the experiment should be much larger than the size of the aggregates in the concrete.

Fig. 17 shows the vertical displacement response to the impact of steel balls of 19mm and 8mm in diameter. The skeletons of these two traces are very similar, especially on the reflections from the void and the bottom of the block. The major difference lies on the oscillations of high frequency in the trace associated with impacting with

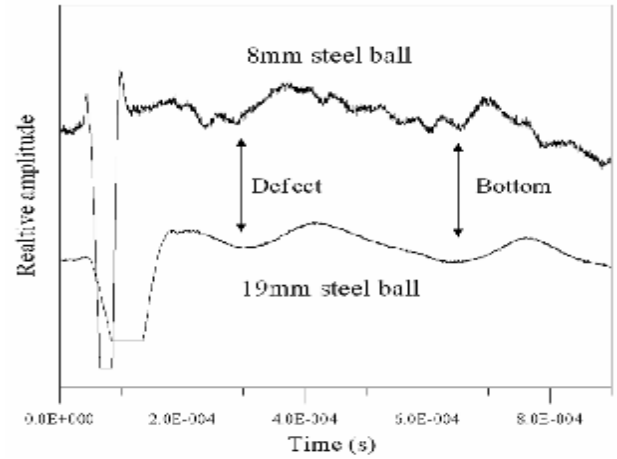

Fig. 17. Comparison of displacement responses of experimental concrete specimen subjected to the impacting of 19mm and an 8mm steel ball.

8mm steel ball. These redundant oscillations really affect the experimental results and smear the resultant image. This phenomenon may be caused by the reflections of elastic waves from the aggregates in the concrete. The maximum size of the aggregates used in the concrete for the experiment is 25mm in diameter. According to Hertz contact theory [21], the impact of a 19mm steel ball on concrete surface may generate elastic waves with the wavelength being about 600mm, 24 times the size of the aggregate. If an 8mm steel ball is used instead, the wavelength is about 250mm, which is 10 times the size of the aggregates. The shorter the wavelength is, the finer the detectable inclusion is. Once the aggregates are detectable by the introduced waves, the results may interfere in detecting the wanted defects such as voids. It is thus concluded that the selection of the steel ball to make the impacting may be very important to have a successful work. The selection should be made on considering the relative magnitude of the wavelength to be introduced and the size of the aggregates.

5. Conclusion

In this paper, a new method integrating the point-source /point-receiver scheme and the SAFT process is proposed to image the defects inside concrete structures. The method utilizes the impact of steel balls to generate elastic waves for searching for the defects implied in concrete and therefore the effective functioning depth is much larger than using the ultrasonic method. Furthermore, the SAFT process could achieve the effect as scanning with a phased array system by post-processing the recorded signals without bulky apparatus. This method extracts useful information from a series of measurements to enhance the

S/N ratio of the image so that the location and the front-end shape of the defects can be more clearly and easily exposed. Another advantage is that only the well developed apparatus basing on elastic wave technology is required to fulfill this method. There is no need to make lots of effort to develop a whole new apparatus for this method. From the study of numerical simulation, the capability of this new method to detect and emerge possible defects in a matrix material by imaging is even clearly proven. As compared to the traditional B-scan diagram, this method can provide better results to identify the number of the defects and their locations, sizes, and front-end shapes. The displacement traces, usually obtained with the traditional elastic-wave-based NDT method, can be used to generate the high quality image if the wavelength of the introduced wave is properly chosen. It is also noted that the a little inaccuracy of the wave velocity used for calculation will not do much harm to the image. This is a good benefit for practical application since certain inaccuracy often occurs in measuring the wave velocity of in-situ concrete, which is a mixture material. The experimental result agrees with the simulation one that the defect can be identified from the image generated by this new NDT method. In addition, the result also reveals the influence of the wavelength on the image quality for in-situ structure inspection. The elastic wave source should be carefully chosen so that the assumption of this imaging method can be satisfied. That is, the wavelength should be much larger than the dimension of the maximum aggregates in the concrete so that the concrete may be much like a homogeneous material. From the results of this study, it can be prudently concluded that this elastic-wave-based NDT method exhibits high potential in inspecting the defects of in-situ concrete structures.

6. Acknowledgement

The authors thank the financial support of this research from the National Science Council of ROC through the grants NSC 93-2211-E-241-011 and NSC 94-2211-E-241-017.

7. References

[1] Malhotra, V. M. and Carino, N. J., "CRC Handbook on Nondestructive Testing of Concrete," *CRC Press, Inc.*, 1991, pp.169-188.

[2] Wu, T. T. and Fang, J. S., "A new method for measuring concrete elastic constants using horizontally polarized conical transducers," *J. Acoust. Soc. Am.*, vol. 101, no.1, pp. 330-336, 1997.

[3] Wu, T. T., Fang, J. S., Liu, G. Y. and Kuo, M. K., "Detection of elastic constants of a concrete specimen using transient elastic waves," *J. Acoust. Soc. Am.*, vol. 98, no. 4, pp. 2142-2148, 1995.

[4] Wu, T. T., Fang, J. S., and Liu, P. L., "Detection of the Depth of a Surface-breaking Crack Using Transient Elastic Waves", *J. Acoust. Soc. Am.*, vol. 97, pp.1678-1686, 1995.

[5] Liu, P.-L., Lee, K.-H, Wu, T.-T., Kuo, M.-K., "Scan of Surface-opening Cracks in Reinforced Concrete Using Transient Elastic Waves", *NDT & E International*, vol. 34, pp. 219-226, 2001.

[6] Carino, N. J., Sansalone, M. and Hsu, N., "A point source point receiver pulse-echo technique for flaw detection in concrete," *ACI Journal*, proceeding, vol. 83, pp.199-208, 1986.

[7] Nazarian, S. and Desai, R., "Automated surface wave method: Field testing," *J. Geotechnical Engineering*, vol. 119, no. 7, pp. 1094-1111, 1993.

[8] Oral Büyüköztürk, "Imaging of Concrete Structures," *NDT & E International*, vol.31, no.4, pp. 233-243, 1998.

[9] Chang, Y.-F., Wang, C.-Y. and Hsieh, C.-H., "Feasibility of Detecting Embedded Cracks in Concrete Structures by Reflection Seismology," *NDT & E International*, vol.34, pp. 39-48, 2001.

[10] Rens, K. L., Transue, D. J. and Schuller, M. P., "Acoustic Tomographic Imaging of Concrete Infrastructure," *Journal of Infrastructure system*, vol.6, no. 1, pp. 15-23, 2000.

[11] Ohtsu, M. and Eatanabe, T., "Stack Imaging of Spectral Amplitudes Based on Impact-echo for flaw Detection," *NDT & E International*, vol.35, pp. 189-196, 2002.

[12] Doctor, S. R., Hall, T. E. and Ried, L. D., "SAFT- The Evolution of a Signal Processing Technology for Ultrasonic Testing," *NDT & E International*, vol. 19, pp. 163-167, 1986.

[13] Waszak, J. and Ludwig, R., "Three-Dimensional Ultrasonic Imaging Employing a Time-Domain Synthetic Aperture Focusing Technique," *IEEE Transactions on Instrumentation and Measurement*, vol. 39, no. 2, pp. 441-444, 1990.

[14] Krause, M., Mielentz, F., Milman, B., Müller, W., Schmitz, V. and Wiggenhauser, H., "Ultrasonic Imaging of Concrete Members Using an Array System," *NDT & E International*, vol.34, pp. 403-408, 2001.

[15] Tong, J.-H., "The Development of Concrete Quality Evaluation System-Automation of Measurement and Wireless Data Transfer," *Key Engineering Materials*, vol. 270-273, pp. 1535-1542, 2004.